JOURNAL OF AGRICULTURAL AND FOOD CHEMISTRY
ARTICLE

J. Agric. Food Chem. 2010, 58, 7641–7648 7641
DOI:10.1021/jf101353c

Induction of Heme Oxygenase 1 and Inhibition of Tumor Necrosis Factor α-Induced Intercellular Adhesion Molecule Expression by Andrographolide in EA.hy926 Cells

Ai-Lin Yu,[†] Chia-Yang Lu,[‡] Tsu-Shing Wang,[§] Chia-Wen Tsai,[†] Kai-Li Liu,[‡,∥] Yi-Ping Cheng,[‡] Hebron C. Chang,[⊥] Chong-Kuei Lii,*[,†] and Haw-Wen Chen*[,†]

[†]Department of Nutrition, China Medical University, Taichung, Taiwan, [‡]Department of Nutrition, Chung Shan Medical University, Taichung, Taiwan, [§]Department of Biomedical Sciences, Chung Shan Medical University, Taichung, Taiwan, [∥]Department of Dietitian, Chung Shan Medical University Hospital, Taichung, Taiwan, and [⊥]Department of Biotechnology, Asia University, Taichung, Taiwan

Andrographolide is the most abundant diterpene lactone in *Andrographis paniculata*, which is widely used as a traditional medicine in Southeast Asia. Heme oxygenase 1 (HO-1) is an antioxidant enzyme encoded by a stress-responsive gene. HO-1 has been reported to inhibit the expression of adhesion molecules in vascular endothelial cells (EC). Intercellular adhesion molecule (ICAM-1) is an inflammatory biomarker that is involved in the adhesion of monocytes to EC. In this study, we investigated the effect of andrographolide on the expression of ICAM-1 induced by tumor necrosis factor α (TNF-α) in EA.hy926 cells and the possible mechanisms involved. Andrographolide (2.5−7.5 μM) inhibited the TNF-α-induced expression of ICAM-1 in a dose-dependent manner and resulted in a decrease in HL-60 cell adhesion to EA.hy926 cells ($p < 0.05$). In parallel, andrographolide significantly induced the expression of HO-1 in a concentration-dependent fashion ($p < 0.05$). Andrographolide increased the rate of nuclear translocation of nuclear factor erythroid 2-related 2 (Nrf2) and induced antioxidant response element-luciferase reporter activity. Transfection with HO-1-specific small interfering RNA knocked down HO-1 expression, and the inhibition of expression of ICAM-1 by andrographolide was significantly reversed. These results suggest that stimulation of Nrf2-dependent HO-1 expression is involved in the suppression of TNF-α-induced ICAM-1 expression exerted by andrographolide.

KEYWORDS: Andrographolide; EA.hy926 cells; heme oxygenase 1; ICAM-1; TNF-α

INTRODUCTION

Current epidemiologic predictions suggest that cardiovascular disease (CVD) is reaching pandemic proportions (*1*), and CVD is the leading cause of death worldwide, accounting for ∼16.7 million deaths each year (*2*). This number is predicted to reach approximately 25 million by 2020, if current trends continue (*3*). The reasons for the increased global incidence of CVD include the aging of the world's population and lifestyles in lower- and middle-income countries becoming more akin to those of wealthier nations (*1*).

CVD is partially characterized by chronic inflammation and an increased level of expression of inflammatory biomarkers, such as intercellular adhesion molecule (ICAM-1), vascular cell adhesion molecule (VCAM-1), and E-selectin, on the surface of the activated endothelial cells (EC) and in the blood circulation (*4*). Increased circulating levels of these adhesion molecules are considered to be predictive of CVD risk because they indicate a proinflammatory state in the vasculature (*4*). In vivo inflammatory processes are mediated by the involvement of proinflammatory mediators, including tumor necrosis factor α (TNF-α), interleukin 6 (IL-6), IL-12, and interferon γ (INF-γ). EC play a key role in coordinating leukocyte trafficking to specific tissues that regulate their activation (*5*). When confronted by an inflammatory stimulus, e.g., bacterial lipopolysaccharide (LPS) (*6*), TNF-α (*7*), or IL-1β (*8*), EC become activated as a result of modification of their phenotype. This is accompanied primarily by the upregulation of a series of proinflammatory genes, e.g., E-selectin, P-selectin, VCAM-1, and ICAM-1 (*6*−*8*). The expression of these genes is regulated primarily by the activation of transcription factor NF-κB (*9*). The proper production of proinflammatory cytokines aids in innate immune responses; however, overproduction causes undesirable side effects such as tissue injury, septic shock, and even death (*10*). To avoid the consequences of uncontrolled production, the expression of proinflammatory genes must be strictly regulated (*11*). One of the mechanisms by which inflammation is counteracted is the expression of the

*To whom correspondence should be addressed. H.-W.C.: Department of Nutrition, China Medical University, Taichung 404, Taiwan; telephone, +886 4 22053366, ext. 7520; fax, +886 4 2206 2891; e-mail, chenhw@mail.cmu.edu.tw. C.-K.L.: Department of Nutrition, China Medical University, Taichung 404, Taiwan; telephone, +886 4 22053366, ext. 7519; fax, +886 4 2206 2891; e-mail, cklii@mail.cmu.edu.tw.

Published on Web 06/10/2010

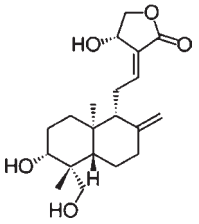

Figure 1. Chemical structure of andrographolide.

anti-inflammatory genes of activated EC. Because of their dual ability to inhibit the expression of proinflammatory genes associated with EC activation and to protect EC from undergoing apoptosis, Bach and colleagues (*11*) referred to these genes as protective genes. Soares et al. (*12*) have hypothesized that the stress-responsive gene encoding heme oxygenase 1 (HO-1) acts in such a manner.

HO-1 is an inducible enzyme that catalyzes the rate-limiting step in the oxidative degradation of free heme into Fe^{2+}, carbon monoxide, and biliverdin, which is subsequently catabolized into bilirubin by biliverdin reductase (*13*). Induction of the gene encoding HO-1 is primarily regulated at the transcriptional level, and transcription factor Nrf2 plays a critical role in the inducibility of the gene (*14*). Under unstimulated conditions, Nrf2 is sequestered in the cytoplasm by binding to Klech-like ECH-associated protein 1 (Keap1) (*15*). This complex is disrupted by several electrophilic antioxidants, and Nrf2 is freed and translocated to the nucleus where it binds to antioxidant response element (ARE) sequences in the HO-1 gene promoter (*16*, *17*). HO-1 can also be induced by its substrate, free heme, and by a diversity of proinflammatory stimuli, which suggests that HO-1 is involved in heme degradation as well as in resolution of inflammation (*18*).

Andrographis paniculata (Burm. f) Nees, a Chinese herb, is a member of the Acanthaceae family. It is widely cultivated in Southeast Asia and is widely used as a traditional medicine in India, China, Thailand, and Scandinavia (*19*). Andrographolide (**Figure 1**) is the most abundant diterpene lactone in the leaves and stems of *A. paniculata* and has high biological activity and therapeutic potential (*20*). Andrographolide has been studied for its anti-inflammatory (*21*−*23*), chemopreventive (*24*), antiangiogenic (*25*), antiproliferative (*26*), and antiapoptotic (*27*) activities. Because of the significant role of inflammation in CVD development, the cardiovascular benefits of andrographolide as the result of its anti-inflammatory activity cannot be ignored.

Therefore, on the basis of the well-known anti-inflammatory activity of andrographolide, this study was designed to explore the effect of andrographolide on the TNF-α-induced expression of ICAM-1 in EAhy.926 cells and the mechanism by which andrographolide acts to influence ICAM-1 expression.

MATERIALS AND METHODS

Materials. Monocytic HL-60 cells were obtained from Bioresources Collection and Research Center (BCRC, Taiwan). Dulbecco's modified Eagle's medium (DMEM), RPMI 1640, 25% trypsin-EDTA, penicillin-streptomycin, RPMI-1640 without phenol red, and OPTI-MEM were from GIBCO/BRL (Grand Island, NY). Fetal bovine serum (FBS) was from HyClone (Logan, UT). 3-(4,5-Dimethylthiazol-2-yl)-2,5-diphenyltetrazolium bromide (MTT), sodium bicarbonate, sodium phosphate dibasic heptahydrate, TNF-α, and all other chemicals were from Sigma (St. Louis, MO). TRIzol reagent was from Invitrogen (Carlsbad, CA). Andrographolide and antibody against HO-1 were from Calbiochem (Darmstadt, Germany). The antibody raised against ICAM-1 was from Cell Signaling Technology (Boston, MA). The antibody raised against Nrf2 was from Santa Cruz Biotechnology (Santa Cruz, CA). The luciferase assay kit was from Promega (Madison, WI). Bis-(carboxyethyl)carboxyfluorescein acetoxymethyl ester (BCECF-AM) was from Molecular Probes (Eugene, OR).

Cell Cultures. The human endothelial cell line EA.hy926 was cultured in DMEM supplemented with 3.7 g/L $NaHCO_3$, 10% FBS, 100 units/mL penicillin, and 100 μg/mL streptomycin at 37 °C in a 5% CO_2 humidified incubator. The HL-60 cells were cultured in T-75 tissue culture flasks in RPMI 1640 medium supplemented with 10% fetal bovine serum, 100000 units/L penicillin, and 100 mg/L streptomycin.

Cell Viability Assay. Cell viability was assessed by the MTT assay. The MTT assay measures the ability of viable cells to reduce a yellow 3-(4,5-dimethylthiazol-2-yl)-2,5-diphenyltetrazolium bromide to a purple formazan by mitochondrial succinate dehydrogenase. EA.hy926 cells were grown to 70−80% confluence and were then treated with different concentrations of andrographolide (0−20 μM) for 16 h followed by incubation with TNF-α (1 ng/mL) for an additional 6 h. Finally, the DMEM medium was removed, and the cells were washed with PBS. The cells were then incubated with MTT (0.5 mg/mL) in DMEM medium at 37 °C for an additional 3 h. The medium was removed, and 2-propanol was added to dissolve the formazan. After centrifugation at 20000*g* for 5 min, the supernatant of each sample was transferred to 96-well plates, and the absorbance was read at 570 nm in an ELISA reader. The absorbance in cultures treated with 0.1% DMSO was regarded as 100% cell viability.

Monocyte Adhesion Assay. EA.hy926 cells in 12-well plates were allowed to grow to 80% confluence and were then pretreated with andrographolide for 16 h followed by incubation with 1 ng/mL TNF-α for an additional 6 h. The human monocytic HL-60 cells cultured in RPMI 1640 medium with 10% FBS were labeled with 1 μM 2,7-bis(2-carboxyethyl)-5(6)-carboxyfluorescein acetoxymethyl ester (BCECF-AM). At the end of the andrographolide and TNF-α treatment, a total of 1×10^6 BCECF-AM-labeled HL-60 cells were added to each well, and the cells were co-incubated with EA.hy926 cells at 37 °C for 30 min. The wells were washed and filled with cell culture medium, and the plates were sealed, inverted, and centrifuged at 100*g* for 5 min to remove nonadherent HL-60 cells. Bound HL-60 cells were lysed in a 1% SDS solution, and the fluorescence intensity was determined in a fluoroscan ELISA plate reader (FLX800, Bio-Tek, Winooski, VT) with an excitation wavelength of 480 nm and an emission wavelength of 520 nm. A control study showed that fluorescence is a linear function of HL-60 cell density in the range of 3000−80000 cells/well. The results are reported on the basis of the standard curve obtained.

Western Blotting Analysis. After each experiment, cells were washed twice with cold PBS and were harvested in 150 μL of lysis buffer [10 mM Tris-HCl (pH 8), 0.1% Triton X-100, 320 mM sucrose, 5 mM EDTA, 1 mM PMSF, 1 mg/L leupeptin, 1 mg/L aprotinin, and 2 mM dithiothreitol]. Cell homogenates were centrifuged at 14000*g* for 20 min at 4 °C. The resulting supernatant was used as a cellular protein for Western blot analysis. The total protein was analyzed by use of the Coomassie Plus protein assay reagent kit (Pierce Biotechnology Inc., Rockford, IL). Equal amounts of cellular proteins were electrophoresed in an sodium dodecyl sulfate−polyacrylamide gel, and proteins were then transferred to polyvinylidene fluoride membranes (Millipore Corp., Bedford, MA). Nonspecific binding sites on the membranes were blocked with 5% nonfat milk in 15 mM Tris/150 mM NaCl buffer (pH 7.4) at room temperature for 2 h. Membranes were probed with rabbit anti-human ICAM-1, HO-1, and β-actin antibodies. The membranes were then probed with the secondary antibody labeled with horseradish peroxidase. The bands were visualized by using an enhanced chemiluminescence kit (PerkinElmer Life Science, Boston, MA) and were quantitated with an ImageGauge (Fuji Film).

RNA Isolation and RT-PCR. Total RNA of EA.hy926 cells was extracted by using Trizol reagent. We used 4 μg of total RNA for the synthesis of first-strand cDNA by using Moloney murine leukemia virus reverse transcriptase (Promega) in a final volume of 20 μL containing 250 ng of oligo-dT and 40 units of RNase inhibitor. PCR was conducted in a thermocycler in a reaction volume of 50 μL containing 20 μL of cDNA, BioTaq PCR buffer, 50 μmol of each deoxyribonucleotide triphosphate, 1.25 mmol/L $MgCl_2$, and 1 unit of BioTaq DNA polymerase (BioLine). Oligonucleotide primers of ICAM-1 (forward, 5′-TGAAGGCCACCC-CAGAGGACAAC-3′; reverse, 5′-CCCATTATGACTGCGGCTG-CTGCTACC-3′), HO-1 (forward, 5′-CTGAGTTCATGAGGAACTTT-CAGAAG-3′; reverse, 5′-TGGTACAGGGAGGCCATCAC-3′), and

glyceraldehyde-3-phosphate dehydrogenase (forward, 5′-CCATCAC-CATCTTCCAGGAG-3′; reverse, 5′-CCTGCTTCACCACCTTCTTG-3′) were designed on the basis of published sequences (*28*, *29*). Amplification of ICAM-1 and GAPDH was achieved when samples were heated to 95 °C for 5 min and then immediately cycled 32 times through a 1 min denaturing step at 94 °C, a 1 min annealing step at 56 °C, and a 1 min elongation step at 72 °C. Amplification of HO-1 and GAPDH was achieved when samples were heated to 95 °C for 5 min and then immediately cycled 39 times through a 1 min denaturing step at 95 °C, a 1 min annealing step at 55 °C, and a 2 min elongation step at 72 °C. The glyceraldehyde-3-phosphate dehydrogenase cDNA level was used as the internal standard. PCR products were resolved in a 1% agarose gel and were scanned by using a Digital Image Analyzer (Alpha Innotech) and quantitated with an ImageGauge.

Plasmids, Transfection, and Luciferase Assays. A p2xARE/Luc fragment containing tandem repeats of double-stranded oligonucleotides spanning the Nrf2 binding site, 5′-TGACTCAGCA-3′, as described by Kataoka et al. (*30*), was introduced into the pGL3 promoter plasmid (Promega). All subsequent transfection experiments were performed by using nanofection reagent (PAA, Austria) according to the manufacturer s instructions. For luciferase assays, the cell lysate was first mixed with a luciferase substrate solution (E1500, Promega), and the resulting luciferase activity was measured by using a microplate luminometer (TROPIX TR-717, Applied Biosystems). For each experiment, luciferase activity was determined in triplicate and was normalized with β-galactosidase activity.

RNA Interference by Small Interfering RNA of HO-1. Predesigned small interfering RNA (siRNA) against human HO-1 and nontargeting control pool siRNA were purchased from Dharmacon Inc. (Lafayette, CO). EA.hy926 cells were transfected with HO-1 siRNA SMARTpool by using DharmaFECT1 transfection reagent (Thermo) according to the manufacturer s instructions. Specific silencing was confirmed by at least three independent immunoblotting assays with cellular extracts 8 h after transfection.

Nuclear Extract Preparation. After each experiment, cells were washed twice with cold PBS and were then scraped from the dishes with 1000 μL of PBS. Cell homogenates were centrifuged at 2000*g* for 5 min. The supernatant was discarded, and the cell pellet was allowed to swell on ice for 15 min after the addition of 200 μL of hypotonic buffer containing 10 mM HEPES, 1 mM $MgCl_2$, 1 mM EDTA, 10 mM KCl, 0.5 mM DTT, 0.5% Nonidet P-40, 4 μg/mL leupeptin, 20 μg/mL aprotinin, and 0.2 mM PMSF. After centrifugation at 7000*g* for 15 min, pellets containing crude nuclei were resuspended in 50 μL of hypertonic buffer containing 10 mM HEPES, 400 mM KCl, 1 mM $MgCl_2$, 0.25 mM EDTA, 0.5 mM DTT, 4 μg/mL leupeptin, 20 μg/mL aprotinin, 0.2 mM PMSF, and 10% glycerol at 4 °C for 30 min. The samples were then centrifuged at 20000*g* for 15 min. The supernatant containing the nuclear proteins was collected and stored at −80 °C until the Western blotting assay.

Statistical Analysis. Data were analyzed by using analysis of variance (SAS Institute, Cary, NC). The significance of the difference between mean values was determined by one-way analysis of variance followed by Tukey's test; p values of < 0.05 were taken to be statistically significant.

RESULTS

Cell Viability. The MTT assay was used to test whether the concentration of andrographolide used in the presence of TNF-α caused cell damage. As shown in **Figure 2**, there were no adverse effects on the growth of EA.hy926 cells up to an andrographolide concentration of 7.5 μM in the presence of 1 ng/mL TNF-α, which was used to induce the expression of ICAM-1. The highest concentration of andrographolide used in this study was 7.5 μM, and thus, the effects of andrographolide observed were not due to its cytotoxicity.

Effect of Andrographolide on the TNF-α-Induced Expression of ICAM-1 in EA.hy926 Cells. EA.hy926 cells were pretreated with 7.5 μM andrographolide for the indicated times before being exposed to 1 ng/mL TNF-α for 6 h. The protein expression of ICAM-1 was significantly suppressed after pretreatment for 4 h compared with that treated with TNF-α alone, and the inhibition was sustained with pretreatment for up to 16 h (**Figure 3A**).

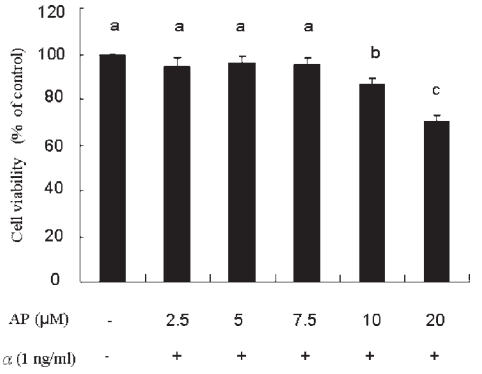

Figure 2. Effect of andrographolide (AP) on the cell viability of EA.hy926 cells in the presence of TNF-α. Cells were pretreated with 0−20 μM andrographolide for 16 h followed by incubation with 1 ng/mL TNF-α for an additional 6 h. Cell viability was measured by using the MTT assay. Values are means ± SD of three independent experiments. Values not sharing the same letter are significantly different ($p < 0.05$).

To determine whether the TNF-α-induced protein and mRNA expression of ICAM-1 were dose-dependently affected by andrographolide, concentrations of andrographolide ranging from 0 to 7.5 μM were studied. As shown in panels **B** and **C** of **Figure 3**, the inhibition of TNF-α-induced protein and mRNA expression of ICAM-1 by andrographolide was dose-dependent. A significant inhibitory effect of andrographolide on ICAM-1 protein expression was observed at concentrations greater than 2.5 μM, and a significant inhibitory effect on ICAM-1 mRNA expression was observed at concentrations greater than 5 μM.

Andrographolide Inhibits HL-60 Cell Adhesion. We next determined whether andrographolide pretreatment could inhibit HL-60 cell adhesion. As shown in **Figure 4**, TNF-α significantly increased the level of HL-60 cell adhesion. However, andrographolide pretreatment inhibited HL-60 cell adhesion in a dose-dependent manner, and significant effects were found at 5 and 7.5 μM.

Effect of Andrographolide on HO-1 Expression of EA.hy926 Cells in the Presence of TNF-α. The stress-responsive gene encoding HO-1 has been recognized to be a protective gene in EC (*12*). To determine whether the inhibition of the TNF-α-induced expression of ICAM-1 by andrographolide was due to upregulation of HO-1, EA.hy926 cells were pretreated with various concentrations of andrographolide for 16 h before being exposed to TNF-α for an additional 6 h. As shown in panels **A** and **B** of **Figure 5**, TNF-α did not affect the protein or mRNA expression of HO-1. However, pretreatment with andrographolide for 16 h significantly enhanced both protein and mRNA expression of HO-1 in a concentration-dependent manner.

Andrographolide Increases the Rate of Nuclear Translocation of Nrf2 and Induces ARE-Luciferase Reporter Activity. Nrf2 is a major transcription factor that regulates ARE-driven gene expression (*31*). We further determined whether Nrf2 is activated by andrographolide. As shown in **Figure 6A**, cells treated with 7.5 μM andrographolide had a higher level of Nrf2 accumulation in the nuclear fraction as early as 1 h, and this accumulation was sustained until 6 h. We used cells transfected with luciferase reporter constructs harboring the ARE to determine the specificity of andrographolide for this sequence. As shown in **Figure 6B**, andrographolide increased ARE-luciferase activity in a dose-dependent manner, and a significant effect was found at 5 and 7.5 μM.

HO-1 siRNA Alleviates Andrographolide Inhibition of ICAM-1 Expression in the Presence of TNF-α. The role of HO-1 in the

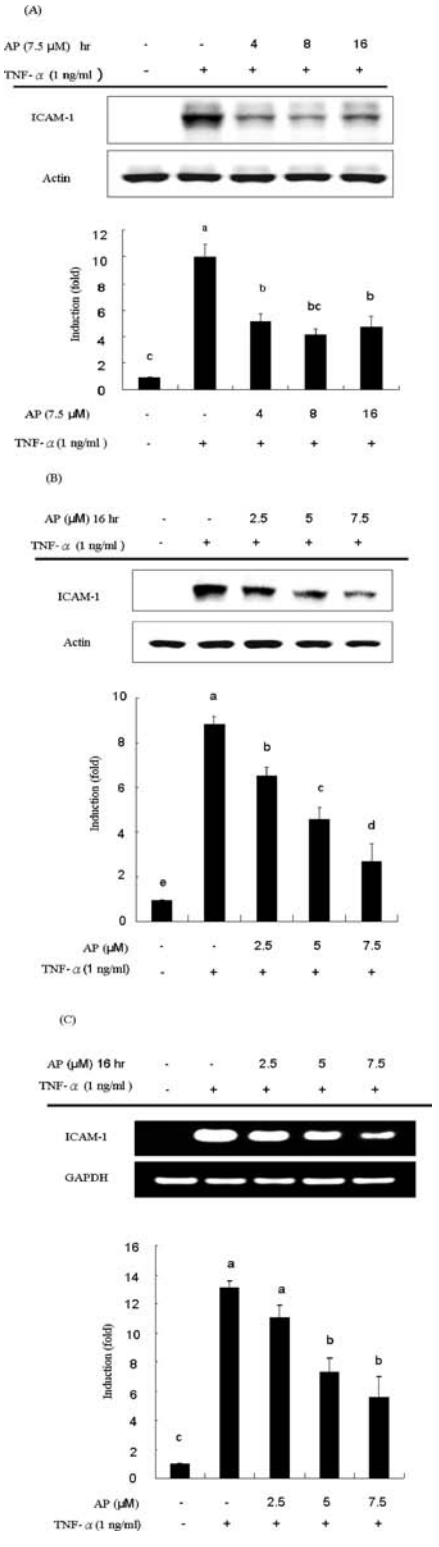

Figure 3. Andrographolide (AP) inhibits TNF-α-induced ICAM-1 expression in EA.hy926 cells. (**A**) Cells were pretreated with 7.5 μM andrographolide for various time periods. (**B**) Cells were pretreated with 0−7.5 μM andrographolide for 16 h followed by incubation with 1 ng/mL TNF-α for an additional 6 h. Aliquots of total protein (20 μg) were used for Western blot analysis. (**C**) Total RNA was isolated from cells and was subjected to RT-PCR with specific ICAM-1 and GAPDH primers as described in Materials and Methods. Values are means ± SD of three independent experiments. Values not sharing the same letter are significantly different ($p < 0$ 0.05). One representative immunoblot from three independent experiments is shown.

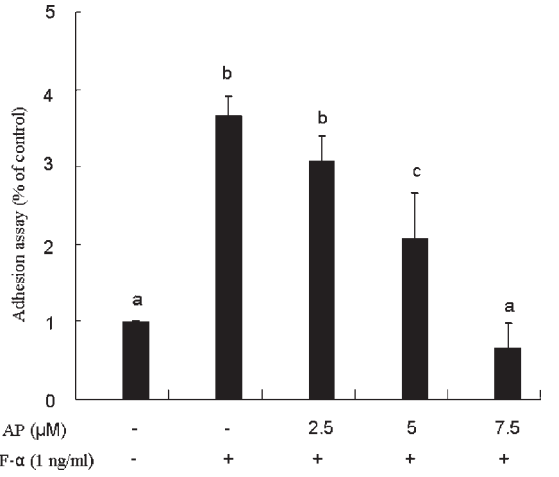

Figure 4. Effect of andrographolide (AP) on TNF-α-induced HL-60 cell adhesion. Cells were pretreated with andrographolide for 16 h before being challenged with 1 ng/mL TNF-α for an additional 6 h. Values are means ± SD of three independent experiments. Values not sharing the same letter are significantly different ($p < 0.05$).

inhibition of ICAM-1 expression by andrographolide in the presence of TNF-α was examined by using an siRNA SMARTpool system to create an HO-1 knockdown model. EA.hy926 cells were transfected with an siHO-1 construct for 8 h, followed by treatment with 7.5 μM andrographolide for 16 h and TNF-α for an additional 6 h. Control cells were transfected with a nontargeting siRNA construct (NC). The efficiency of the siRNA SMARTpool system in knocking down HO-1 was assayed by Western blot and RT-PCR assay (**Figure 7A**). HO-1 siRNA alleviated the andrographolide inhibition of protein (**Figure 7B**) and the mRNA expression (**Figure 7C**) of ICAM-1 in the presence of TNF-α. These results imply the importance of HO-1 for the inhibition of TNF-α-induced ICAM-1 expression by andrographolide.

DISCUSSION

In this study, we have demonstrated that andrographolide, an active phytocompound of *A. paniculata*, effectively suppressed ICAM-1 expression in vascular EC exposed to TNF-α and that this protection is likely associated with Nrf2-dependent HO-1 induction.

A. paniculata is widely used in Asia to treat infection, inflammation, cold, fever, and diarrhea and as an antidote to snakebite (*32*). The anti-inflammatory activities of *A. paniculata* and of andrographolide, the most abundant diterpene lactone in *A. paniculata*, have been extensively studied. The concentrations of andrographolide used (2.5−7.5 μM) in this study are approximately equivalent to those achieved in subjects ingesting *A. paniculata* (*33*). The highest concentration of andrographolide used was 7.5 μM because the MTT results showed that concentrations greater than this caused cell damage in the presence of 1 ng/mL TNF-α (**Figure 2**). These results were consistent with those of a previous study (*34*). According to the cell viability and anti-inflammatory results, andrographolide exhibited a narrow therapeutic window. It would be prudent to use *A. paniculata* and its bioactive compound, andrographolide.

Inhibition of the abnormal induction of adhesion molecules is believed to be one of the mechanisms attributed to the CVD protection of a diversity of phytochemicals, e.g., diallyl disulfide (DADS), diallyl trisulfide (DATS), apigenin, luteolin, and cinnamaldehyde (*35*−*37*). The suppression of ox-LDL-induced E-selectin and VCAM-1 expression by DADS and DATS and,

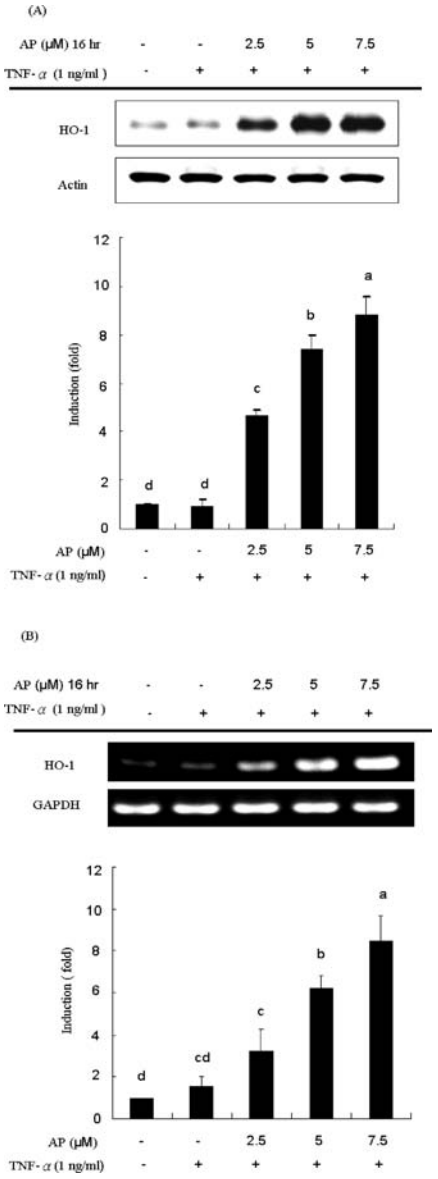

Figure 5. Andrographolide (AP) induces HO-1 expression in EA.hy926 cell. Cells were pretreated with andrographolide for 16 h followed by incubation with TNF-α for an additional 6 h. (**A**) Aliquots of the total protein (20 μg) were used for Western blot analysis. (**B**) Total RNA was isolated from cells and was subjected to RT-PCR with specific HO-1 and GAPDH primers as described in Materials and Methods. Values are means ± SD of three independent experiments. Values not sharing the same letter are significantly different ($p < 0.05$). One representative immunoblot from three independent experiments is shown.

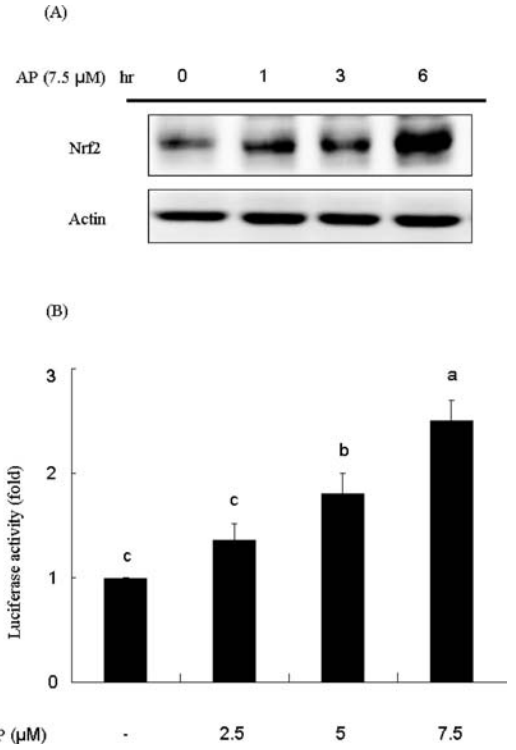

Figure 6. Effect of andrographolide (AP) on Nrf2 nuclear translocation and ARE-luciferase reporter activity. (**A**) Nuclear extracts from cells were prepared after treatment with 7.5 μM andrographolide for the indicated time periods. Immunoblots of nuclear extracts from treated cells were then probed with the Nrf2-specific antibody. (**B**) Cells were transfected with the ARE-luciferase construct (ARE), after 12 h were maintained in low-serum medium for a further 1 h, and were then stimulated with 0−7.5 μM andrographolide for an additional 24 h. The cells were then lysed and analyzed for luciferase activity. Induction is shown as an increase in the normalized luciferase activity in the treated cells relative to the control. Values not sharing the same letter are significantly different ($p < 0.05$). One representative immunoblot from three independent experiments is shown.

thus, monocyte adhesion to EC is likely dependent on the PI3K/PKB or PKA/CREB signaling pathway in an adhesion molecule-specific manner (*35*). The reactive oxygen species scavenging capabilities of apigenin and luteolin proceed dose-dependently in the presence of ox-LDL (*36*). The inhibitory effects of apigenin and luteolin on ICAM-1 and E-selctin expression are, at least partially, attributed to their antioxidant activity and modulation of the PI3K/Akt signaling pathway. In TNF-α-treated EA.hy926 cells, pretreatment with cinnamaldehyde inhibits the expression of ICAM-1 and VCAM-1 and results in the suppression of the adherence of monocytes to EC (*37*).

The essential role of ICAM-1 in mediating the adhesion of WEHI 274.1 cells to ox-LDL-stimulated mouse aortic endothelium was demonstrated in a previous study (*38*). In the study presented here, inhibition of ICAM-1 expression by andrographolide resulted in the suppression of adhesion of HL-60 cells to TNF-α-stimulated EA.hy926 cells (**Figure 4**). The suppressive pattern was dose-dependent, and a significant effect was observed at 5 and 7.5 μM. These results suggest that inhibition of ICAM-1 expression by andrographolide contributes to the suppression of the adhesion of monocytes to inflammatory EC.

The importance of TNF-α in the expression of adhesion molecules has been well recognized, and the role of TNF-α in CVD has been demonstrated in vivo. Mice in which the TNF-α gene is disrupted develop significantly fewer atherosclerotic lesions in the proximal aorta than do their normal counterparts (*39*). The role of NF-κB in the TNF-α-induced expression of cell adhesion molecules has been convincingly demonstrated (*40*). NF-κB is a transcription factor that resides in the cytoplasm under unstimulated circumstances in an inactive form via its association with I-κB. After stimulation with pro-inflammatory agents, I-κB undergoes proteolytic degradation and frees NF-κB. Freed NF-κB translocates from the cytoplasm to the nucleus where it activates target gene transcription (*41*).

The transcriptional activation of genes encoding various antioxidant enzymes and phase II detoxifying enzymes such as HO-1 is regulated by the ARE (*42*). Andrographolide increased the rate of nuclear translocation of Nrf2 and induced ARE-luciferase activity (**Figure 6A,B**), which suggests that andrographolide may

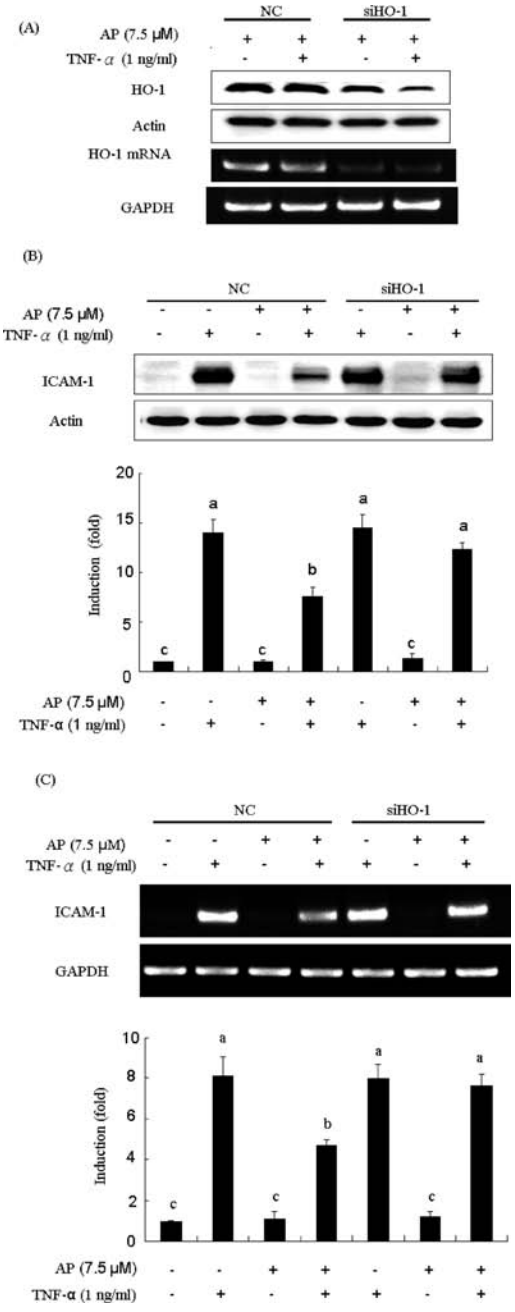

Figure 7. Effect of HO-1 siRNA on the inhibition of ICAM-1 expression by andrographolide (AP). An HO-1 siRNA system was used to silence HO-1 mRNA in cells and to create an siRNA knockdown EA.hy926 cell model. (**A**) Western blot and RT-PCR analyses of HO-1 expression in EA.hy926 cells transfected with HO-1 siRNA. (**B**) Aliquots of total protein (20 μg) were used for Western blot analysis. (**C**) Total RNA was isolated from cells and was subjected to RT-PCR with specific ICAM-1 and GAPDH primers. Values are means ± SD of three independent experiments. Values not sharing the same letter are significantly different ($p < 0$ 0.05). One representative immunoblot from three independent experiments is shown.

induce the expression of ARE-regulated genes. The Keap1/Nrf2/ARE signaling pathway is thought to play an important role in protecting cells from endogenous and exogenous stresses (*43*). In this study, andrographolide induced the expression of HO-1 through the Nrf2/ARE signaling pathway.

Although both in vivo and in vitro studies have demonstrated the potent anti-inflammatory activity of *A. paniculata* and andrographolide (*44*, *45*), the mechanism by which andrographolide acts to prevent adhesion molecule expression is not clear. HO-1 is an inducible enzyme that catalyzes the rate-limiting step in the oxidative degradation of free heme into Fe^{2+}, carbon monoxide, and biliverdin and is regarded as an important cellular antioxidant enzyme. Because of its antioxidant characteristics, HO-1 has been reported to inhibit the expression of adhesion molecules in EC via the generation of bilirubin and the decrease in the level of intracellular free Fe^{2+} (*12*). Additionally, Lee et al. (*46*) indicated that the inhibition of TNF-α-induced adhesion molecule expression by overexpression of HO-1 is associated with the reduced level of formation of a TNFR1−c-Src−$p47^{phox}$ complex and subsequent inhibition of NF-κB activation. Furthermore, inhibition of RelA phosphorylation at Ser^{276} by HO-1 is considered to be involved in suppression of ICAM-1 expression associated with EC activation (*47*). We did not measure the direct effect of siHO-1 on NF-κB activation in this study. Brunt et al. (*48*) found that overexpression of HO-1 reduced NF-κB promoter activity and NF-κB DNA binding activity in response to H_2O_2 in HL-1 cardiomyocytes. Their results might suggest the possibility that andrographolide inhibits TNFα-induced ICAM-1 expression is via suppression of NF-κB activation by HO-1 overexpression in our study. The blockage of the degradation of the inhibitory protein inhibitor κB (I-κB) and the induction of the expression of Nrf2-mediated HO-1 have been shown to make up the working mechanism by which cinnamaldehyde abolishes TNF-α-induced ICAM-1 and VCAM-1 transcription. Recently, HO-1 gene transcription was noted to be induced by one kind of diterpene carnosol via activation of the Nrf2/ARE pathway in PC12 cells (*49*). Andrographolide is a phytocompound with a diterpene structure. On the basis of these findings, the possibility that the inhibition of ICAM-1 expression by andrographolide is via its induction of HO-1 transcription cannot be excluded. In this study, our results revealed that andrographolide dose-dependently inhibited TNF-α-induced protein expression of ICAM-1 in EA.hy926 cells (**Figure 3B**). In contrast with the suppression of ICAM-1 expression, however, HO-1 was dose-dependently upregulated by andrographolide (**Figure 5A,B**). The importance of HO-1 in

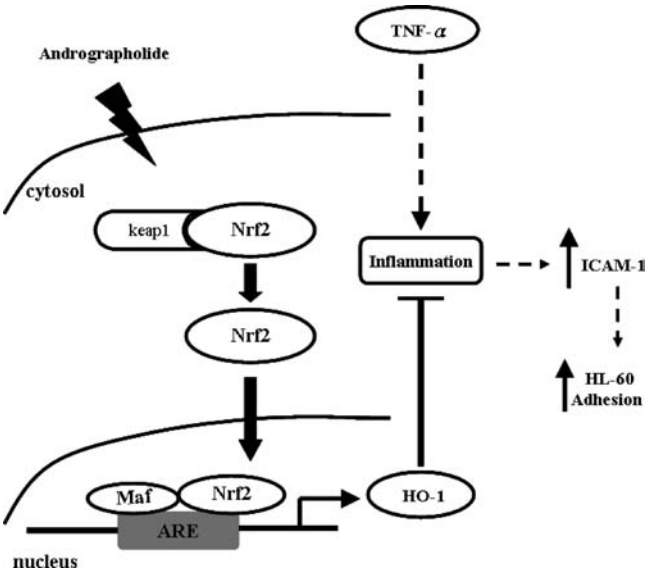

Figure 8. Model showing pathways that mediate the inhibition of expression of ICAM-1 and adhesion of HL-60 cells to EA.hy926 cells by andrographolide under inflammatory conditions. Andrographolide causes the dissociation of Nrf2 from Keap1 and its nuclear translocation. Nrf2 then binds to the ARE, which leads to an induction of HO-1 expression and inhibits ICAM-1 expression and subsequent HL-60 cell adhesion.

the inhibition of ICAM-1 expression was further confirmed by using HO-1 siRNA. In cells transfected with siHO-1, the inhibition of TNF-α-induced ICAM-1 expression by andrographolide was abolished (**Figure 7B,C**). The PI3K/Akt, MAPK, and PKCδ pathways have been reported to be involved in HO-1 expression induced by a variety of phytochemicals (*50*−*52*). We demonstrated in this study that andrographlide induces HO-1 expression. However, signaling pathways involved in nuclear translocation of Nrf2 were not determined, and they are under investigation.

The findings of this study are schematically presented in **Figure 8**. Stimulation of HO-1 by andrographolide is involved in the inhibition of expression of ICAM-1 and the subsequent adhesion of monocytes to EA.hy926 cells. Induction of expression of HO-1 by andrographolide occurs through the Nrf2/ARE signaling pathway. The anti-inflammatory activity of andrographolide confers *A. paniculata* with CVD-protective potential.

ABBREVIATIONS USED

AP, andrographolide; ARE, antioxidant response element; CVD, cardiovascular disease; EC, endothelial cells; HO-1, heme oxygenase 1; ICAM-1, intercellular adhesion molecule; IL, interleukin; Keap 1, Klech-like ECH-associated protein 1; LPS, lipopolysaccharide; Nrf2, nuclear factor erythroid 2-related 2; SD, standard deviation; siRNA, small interfering RNA; TNF-α, tumor necrosis factor α; VCAM-1, vascular cell adhesion molecule.

LITERATURE CITED

(1) Dahlöf, B. Cardiovascular disease risk factors: Epidemiology and risk assessment. *Am. J. Cardiol.* **2010**, *105* (Suppl. 1), 3A–9A.

(2) American Heart Association. International Cardiovascular Disease Statistics. 2007 Update. http://www.americanheart.org/presenter.jhtml?identifier_3001008. Accessed December 10, 2007.

(3) Yach, D.; Hawkes, C.; Gould, C. L.; Hofman, K. J. The global burden of chronic diseases: Overcoming impediments to prevention and control. *J. Am. Med. Assoc.* **2004**, *291*, 2616–2620.

(4) Hwang, S. J.; Ballantyne, C. M.; Sharrett, A. R.; Smith, L. C.; Davis, C. E.; Gotto, A. M., Jr.; Boerwinkle, E. Circulating adhesion molecules VCAM-1, ICAM-1, and E-selectin in carotid atherosclerosis and incident coronary heart disease cases: The Atherosclerosis Risk In Communities (ARIC) study. *Circulation* **1997**, *96*, 4219–4225.

(5) Cines, D. B.; Pollak, E. S.; Buck, C. A.; Loscalzo, J.; Zimmerman, G. A.; McEver, R. P.; Pober, J. S.; Wick, T. M.; Konkle, B. A.; Schwartz, B. S.; Barnathan, E. S.; McCrae, K. R.; Hug, B. A.; Schmidt, A. M.; Stern, D. M. Endothelial cells in physiology and in the pathophysiology of vascular disorders. *Blood* **1998**, *91*, 3527–3561.

(6) Hortelano, S.; López-Fontal, R.; Través, P. G.; Villa, N.; Grashoff, C.; Boscá, L.; Luque, A. ILK mediates LPS-induced vascular adhesion receptor expression and subsequent leukocyte trans-endothelial migration. *Cardiovasc. Res.* **2010**, *86*, 283–292.

(7) Oh, J. H.; Park, E. J.; Park, J. W.; Lee, J.; Lee, S. H.; Kwon, T. K. A novel cyclin-dependent kinase inhibitor down-regulates tumor necrosis factor-α (TNF-α)-induced expression of cell adhesion molecules by inhibition of NF-κB activation in human pulmonary epithelial cells. *Int. Immunopharmacol.* **2010**, *10*, 572–579.

(8) Chang, W. C.; Chen, C. H.; Lee, M. F.; Chang, T.; Yu, Y. M Chlorogenic acid attenuates adhesion molecules upregulation in IL-1β-treated endothelial cells. *Eur. J. Nutr.* **2009**, (in press).

(9) Haddad, O.; Chotard-Ghodsnia, R.; Verdier, C.; Duperray, A. Tumor cell/endothelial cell tight contact upregulates endothelial adhesion molecule expression mediated by NFκB: Differential role of the shear stress. *Exp. Cell Res.* **2010**, *316*, 615–626.

(10) zAstiz, M. E.; Rackow, E. C. Septic shock. *Lancet* **1998**, *351*, 1501–1505.

(11) Bach, F. H.; Hancock, W. W.; Ferran, C. Protective genes expressed in endothelial cells: A regulatory response to injury. *Immunol. Today* **1997**, *18*, 483–486.

(12) Soares, M. P.; Seldon, M. P.; Gregoire, I. P.; Vassilevskaia, T.; Berberat, P. O.; Yu, J.; Tsui, T. Y.; Bach, F. H. Heme oxygenase-1 modulates the expression of adhesion molecules associated with endothelial cell activation. *J. Immunol.* **2004**, *172*, 3553–3563.

(13) Ryter, S. W.; Tyrrell, R. M. The heme synthesis and degradation pathways: Role in oxidant sensitivity: Heme oxygenase has both pro- and antioxidant properties. *Free Radical Biol. Med.* **2000**, *28*, 289–309.

(14) Alam, J.; Cook, J. L. Transcriptional regulation of the heme oxygenase-1 gene via the stress response element pathway. *Curr. Pharm. Des.* **2003**, *9*, 2499–2511.

(15) Itoh, K.; Tong, K. I.; Yamamoto, M. Molecular mechanism activating Nrf-2-keap1 pathway in regulation of adaptive response to electrophiles. *Free Radical Biol. Med.* **2004**, *36*, 1208–1213.

(16) Kang, A. N.; Owuor, E.; Yu, R.; Hebbar, V.; Chen, C.; Hu, R.; Mandlekar, S. Induction of xenobiotic enzymes by the MAP kinase pathway and the antioxidant or electrophile response element (ARE/EpRE). *Drug Metab. Rev.* **2001**, *33*, 255–271.

(17) Owuor, E. D.; Kang, A. N. Antioxidants and oxidants regulated signal transduction pathways. *Biochem. Pharmacol.* **2002**, *64*, 765–770.

(18) Willoughby, D. A.; Moore, A. R.; Colville-Nash, P. R.; Gilroy, D. Resolution of inflammation. *Int. J. Immunopharmacol.* **2000**, *22*, 1131–1135.

(19) Bhan, M. K.; Dhar, A. K.; Khan, S.; Lattoo, S. K.; Gupta, K. K.; Choudhary, D. K. Screening and optimization of *Andrographis paniculata* (Burm. f.) Nees for total andrographolide content, yield and its components. *Sci. Hortic.* **2006**, *107*, 386–391.

(20) Singha, P. K.; Roy, S.; Dey, S. Protective activity of andrographolide and arabinogalactan proteins from *Andrographis paniculata* Nees. against ethanol-induced toxicity in mice. *J. Ethnopharmacol.* **2007**, *111*, 13–21.

(21) Habtemariam, S. Andrographolide inhibits the tumour necrosis factor-α-induced upregulation of ICAM-1 expression and endothelial-monocyte adhesion. *Phytother. Res.* **1998**, *12*, 37–40.

(22) Chiou, W. F.; Chen, C. F.; Lin, J. J. Mechanisms of suppression of inducible nitric oxide synthase (iNOS) expression in Raw264.7 cells by andrographolide. *Br. J. Pharmacol.* **2000**, *129*, 1553–1560.

(23) Xia, Y. F.; Ye, B. Q.; Li, Y. D.; Wang, J. G.; He, X. J.; Lin, X.; Yao, X.; Ma, D.; Slungaard, A.; Hebbel, R. P.; Key, N. S.; Geng, J. G. Andrographolide attenuates inflammation by inhibition of NF-kB activation through covalent modification of reduced cysteine 62 of p50. *J. Immunol.* **2004**, *173*, 4207–4217.

(24) Chang, K. T.; Lii, C. K.; Tsai, C. W.; Yang, A. J.; Chen, H. W. Moddulation of the expression of the pi class of glutathione S-transferase by *Andrographis paniculata* extracts and andrographolide. *Food Chem. Toxicol.* **2008**, *46*, 1079–1088.

(25) Sheeja, K.; Guruvayoorappan, C.; Kuttan, G. Antiangiogenic activity of *Andrographis paniculata* extract and andrographolide. *Int. Immunopharmacol.* **2007**, *7*, 211–221.

(26) Cheung, H. Y.; Cheung, S. H.; Li, J.; Cheung, C. S.; Lai, W. P.; Fong, W. F.; Leung, F. M. Andrographolide isolated from andrographis paniculata induces cell cycle arrest and mitochondrial-mediated apoptosis in human leukemic HL-60 cells. *Planta Med.* **2005**, *71*, 1106–1111.

(27) Zhao, F.; He, E. Q.; Wang, L.; Liu, K. Anti-tumor activities of a diterpene from *Andrographis paniculata*, by inducing apoptosis and inhibiting VEGF level. *J. Asian Nat. Prod. Res.* **2008**, *10*, 467–473.

(28) Meagher, L.; Mahiouz, D.; Sugars, K.; Burrows, N.; Norris, P.; Yarwood, H.; Becker-Andre, M.; Haskard, D. O. Measurement of mRNA for E-selectin, VCAM-1 and ICAM-1 by reverse transcription and the polymerase chain reaction. *J. Immunol. Methods* **1994**, *175*, 237–246.

(29) Sun, X.; Pi, J.; Liu, W.; Hudson, L. G.; Liu, K. J.; Feng, C. Induction of heme oxygenase 1 by arsenite inhibits cytokine-induced monocyte adhesion to human endothelial cells. *Toxicol. Appl. Pharmacol.* **2009**, *236*, 202–209.

(30) Kataoka, K.; Handa, H.; Nishizawa, M. Induction of cellular anti-oxidative stress genes through heterodimeric transcription factor Nrf2/small Maf by antirheumatic gold(I) compounds. *J. Biol. Chem.* **2001**, *276*, 34074–34081.

(31) Nguyen, T.; Yang, C. S.; Pickett, C. B. The pathways and molecular mechanisms regulating Nrf2 activation in response to chemical stress. *Free Radical Biol. Med.* **2004**, *37*, 433–441.
(32) Roxas, M.; Jurenka, J. Colds and influenza: A review of diagnosis and conventional, botanical and nutritional considerations. *Altern. Med. Rev.* **2007**, *12*, 25–48.
(33) Panossian, A.; Hovhannisyan, A.; Mamikonyan, G.; Abrahamian, H.; Hambardzumyan, E.; Gabrielian, E.; Goukasova, G.; Wikman, G.; Wagner, H. Pharmacokinetic and oral bioavailability of andrigrapholide from *Andrographis paniculata* fixed combination Kan Jang in rats and human. *Phytomedicine* **2000**, *7*, 351–364.
(34) Lee, Y. C.; Lin, H. H.; Hsu, C. H.; Wang, C. J.; Chiang, T. A.; Chen, J. H. Inhibitory effects of andrographolide on migration and invasion in human non-small cell lung cancer A549 cells via down-regulation of PI3K/Akt signaling pathway. *Eur. J. Pharmacol.* **2010**, *632*, 23–32.
(35) Lei, Y. P.; Chen, H. W.; Sheen, L. Y.; Lii, C. K. Diallyl disulfide and diallyl trisulfide suppress oxidized LDL-induced vascular cell adhesion molecule and E-selectin expression through protein kinase A- and B-dependent signaling pathways. *J. Nutr.* **2008**, *138*, 996–1003.
(36) Lii, C. K.; Lei, Y. P.; Yao, H. T.; Hsieh, Y. S.; Tsai, C. W.; Liu, K. L.; Chen, H. W. *Chrysanthemum morifolium* Ramat. reduces the oxidized LDL-induced expression of intercellular adhesion molecule-1 and E-selectin in human umbilical vein endothelial cells. *J. Ethnopharmacol.* **2010**, *128*, 213–220.
(37) Liao, B. C.; Hsieh, C. W.; Liu, Y. C.; Tzeng, T. T.; Sun, Y. W.; Wung, B. S. Cinnamaldehyde inhibits the tumor necrosis factor-α-induced expression of cell adhesion molecules in endothelial cells by suppressing NF-κB activation: Effects upon IκB and Nrf2. *Toxicol. Appl. Pharmacol.* **2008**, *229*, 161–171.
(38) Kevil, C. G.; Patel, R. P.; Bullard, D. C. Essential role of ICAM-1 in mediating monocyte adhesion to aortic endothelial cells. *Am. J. Physiol.* **2001**, *281*, C1442–C1447.
(39) Ohta, H.; Wada, H.; Niwa, T.; Kirii, H.; Iwamoto, N.; Fujii, H.; Saito, K.; Sekikawa, K.; Seishima, M. Disruption of tumor necrosis factor-α gene diminishes the development of atherosclerosis in ApoE-deficient mice. *Atherosclerosis* **2005**, *180*, 11–17.
(40) Denk, A.; Goebeler, M.; Schmid, S.; Berberich, I.; Ritz, O.; Lindemann, D.; Ludwig, S.; Wirth, T. Activation of NF-κB via the I-κB kinase complex is both essential and sufficient for proinflammatory gene expression in primary endothelial cells. *J. Biol. Chem.* **2001**, *276*, 28451–28458.
(41) Gaur, U.; Aggarwal, B. B. Regulation of proliferation, survival and apoptosis by members of the TNF superfamily. *Biochem. Pharmacol.* **2003**, *66*, 1403–1408.
(42) Kim, K. M.; Jung, D. H.; Jang, D. S.; Kim, Y. S.; Kim, J. M.; Kim, H. N.; Surh, Y. J.; Kim, J. S. Puerarin suppresses AGEs-induced inflammation in mouse mesangial cells: A possible pathway through the induction of heme oxygenase-1 expression. *Toxicol. Appl. Pharmacol.* **2010**, *244*, 106–113.
(43) Kensler, T. W.; Wakabayashi, N.; Biswal, S. Cell survival responses to environmental stresses via the Keap1-Nrf2-ARE pathway. *Annu. Rev. Pharmacol. Toxicol.* **2007**, *47*, 89–116.
(44) Chao, W. W.; Kuo, Y. H.; Hsieh, S. L.; Lin, B. F. Inhibitory effects of ethyl acetate extract of *Andrographis paniculata* on NF-κB transactivation activity and LPS-induced acute inflammation in mice. *Evidence-Based Complement Altern. Med.* **2009**, (in press).
(45) Chao, W. W.; Kuo, Y. H.; Lin, B. F. Anti-inflammatory Activity of New Compounds from *Andrographis paniculata* by NF-κB Transactivation Inhibition. *J. Agric. Food Chem.* **2010**, *58*, 2505–2512.
(46) Lee, I. T.; Luo, S. F.; Lee, C. W.; Wang, S. W.; Lin, C. C.; Chang, C. C.; Chen, Y. L.; Chau, L. Y.; Yang, C. M. Overexpression of HO-1 protects against TNF-α-mediated airway inflammation by down-regulation of TNFR1-dependent oxidative stress. *Am. J. Pathol.* **2009**, *175*, 519–532.
(47) Seldon, M. P.; Silva, G.; Pejanovic, N.; Larsen, R.; Gregoire, I. P.; Filipe, J.; Anrather, J.; Soares, M. P. Heme oxygenase-1 inhibits the expression of adhesion molecules associated with endothelial cell activation via inhibition of NF-κB RelA phosphorylation at serine 276. *J. Immunol.* **2007**, *179*, 7840–7851.
(48) Brunt, K. R.; Tsuji, M. R.; Lai, J. H.; Kinobe, R. T.; Durante, W.; Claycomb, W. C.; Ward, C. A.; Melo, L. G. Heme oxygenase-1 inhibits pro-oxidant induced hypertrophy in HL-1 cardiomyocytes. *Exp. Biol. Med.* **2009**, *234*, 582–594.
(49) Martin, D.; Rojo, A. I.; Salinas, M.; Diaz, R.; Gallardo, G.; Alam, J.; De Galarreta, C. M.; Cuadrado, A. Regulation of heme oxygenase-1 expression through the phosphatidylinositol 3-kinase/Akt pathway and the Nrf2 transcription factor in response to the antioxidant phytochemical carnosol. *J. Biol. Chem.* **2004**, *279*, 8919–8929.
(50) Gong, P.; Hu, B.; Cederbaum, A. I. Diallyl sulfide induces heme oxygenase-1 through MAPK pathway. *Arch. Biochem. Biophys.* **2004**, *432*, 252–260.
(51) Balogun, E.; Hoque, M.; Gong, P.; Killeen, E.; Green, C. J.; Foresti, R.; Alam, J.; Motterlini, R. Curcumin activates the haem oxygenase-1 gene via regulation of Nrf2 and the antioxidant-responsive element. *Biochem. J.* **2003**, *371* (Part 3), 888–895.
(52) Kim, K. M.; Jung, D. H.; Jang, D. S.; Kim, Y. S.; Kim, J. M.; Kim, H. N.; Surh, Y. J.; Kim, J. S. Puerarin suppresses AGEs-induced inflammation in mouse mesangial cells: A possible pathway through the induction of heme oxygenase-1 expression. *Toxicol. Appl. Pharmacol.* **2010**, *244*, 106–113.

Received for review April 10, 2010. Revised manuscript received May 25, 2010. Accepted May 26, 2010. This work was supported by Grant CMU98-CT-21.